J|A|C|S
ARTICLES

Published on Web 07/06/2009

Hydrogenation of the α,β-Unsaturated Aldehydes Acrolein, Crotonaldehyde, and Prenal over Pt Single Crystals: A Kinetic and Sum-Frequency Generation Vibrational Spectroscopy Study

Christopher J. Kliewer, Marco Bieri, and Gabor A. Somorjai*

Department of Chemistry, University of California, Berkeley, California 94720, and Materials Sciences Division, Lawrence Berkeley National Laboratory, Berkeley, California 94720

Received November 26, 2008; E-mail: somorjai@socrates.berkeley.edu

Abstract: Sum-frequency generation vibrational spectroscopy (SFG-VS) and kinetic measurements using gas chromatography have been used to study the surface reaction intermediates during the hydrogenation of three α,β-unsaturated aldehydes, acrolein, crotonaldehyde, and prenal, over Pt(111) at Torr pressures (1 Torr of aldehyde, 100 Torr of hydrogen) in the temperature range of 295−415 K. SFG-VS data showed that acrolein has mixed adsorption species of η_2-di-σ(CC)-trans, η_2-di-σ(CC)-cis as well as highly coordinated η_3 or η_4 species. Crotonaldehyde adsorbed to Pt(111) as η_2 surface intermediates. SFG-VS during prenal hydrogenation also suggested the presence of the η_2 adsorption species and became more highly coordinated as the temperature was raised to 415 K, in agreement with its enhanced C=O hydrogenation. The effect of catalyst surface structure was clarified by carrying out the hydrogenation of crotonaldehyde over both Pt(111) and Pt(100) single crystals while acquiring the SFG-VS spectra in situ. Both the kinetics and SFG-VS showed little structure sensitivity. Pt(100) generated more decarbonylation "cracking" product while Pt(111) had a higher selectivity for the formation of the desired unsaturated alcohol, crotyl alcohol.

1. Introduction

The selective hydrogenation of an unsaturated C=C bond in the presence of a C=O carbonyl group of the same molecule has been the subject of much research in recent years. Both experimental and theoretical work has been devoted to this topic and comprehensive reviews of the subject have been published.[1−4] One product of this reaction, the unsaturated alcohol, is an important intermediate in both the pharmaceutical and fragrance industries. However, it is quite difficult to achieve a high selectivity and activity for the unsaturated alcohol product because the hydrogenation of the C=C is thermodynamically preferred by roughly 35 kJ/mol[2].

The platinum group metals are the catalysts most frequently employed during this reaction, but the selectivity for the desired unsaturated alcohol is relatively low for these catalysts. Over platinum, the selectivity for unsaturated alcohol has been shown to improve upon alloying with another metal,[5] for instance Fe[6] or Sn[7], as well as upon the addition of various promoters,[3,8] such as potassium on the surface. Catalyst structure, such as the (111) or (100) crystal face of a metal, has also been suggested to play a role in the reaction selectivity.[9]

Scheme 1. Hydrogenation Pathways for Acrolein

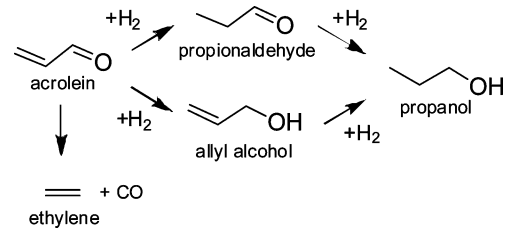

Also effecting the selectivity in the hydrogenation of α,β-unsaturated aldehydes is the amount of steric hindrance to adsorption added to the C=C bond by the placement of bulky groups, such as phenyl or methyl groups, on this side of the molecule. Hoang-Van et al.[10] reported on the hydrogenation of acrolein over various platinum catalysts. Each of the widely used Pt based catalysts (Pt black, Pt−Al, Pt−Si) showed greater than 99% selectivity for the hydrogenation of the C=C to yield propionaldehyde (Scheme 1). In comparison, for the hydrogenation of prenal, the same molecule as acrolein with two methyl groups added to the C=C bond, Birchem et al.[7,11] show at 353 K the dominant product to be the unsaturated alcohol, a complete reversal of the selectivity seen for acrolein hydrogenation.

In this work, the hydrogenation of acrolein, crotonaldehyde, and prenal (Schemes 1−3) was carried out over Pt(111) while

(1) Gallezot, P.; Richard, D. *Catal. Rev.—Sci. Eng.* **1998**, *40*, 81–126.
(2) Maki-Arvela, P.; Hajek, J.; Salmi, T.; Murzin, D. Y. *Appl. Catal., A* **2005**, *292*, 1–49.
(3) Ponec, V. *Appl. Catal., A* **1997**, *149*, 27–48.
(4) Claus, P. *Top. Catal.* **1998**, *5*, 51–62.
(5) Englisch, M.; Ranade, V. S.; Lercher, J. A. *J. Mol. Catal. A* **1997**, *121*, 69–80.
(6) Beccat, P.; Bertolini, J. C.; Gauthier, Y.; Massardier, J.; Ruiz, P. *J. Catal.* **1990**, *126*, 451–456.
(7) Birchem, T.; Pradier, C. M.; Berthier, Y.; Cordier, G. *J. Catal.* **1996**, *161*, 68–77.
(8) Marinelli, T.; Ponec, V. *J. Catal.* **1995**, *156*, 51–59.
(9) Englisch, M.; Jentys, A.; Lercher, J. A. *J. Catal.* **1997**, *166*, 25–35.
(10) Hoang-Van, C.; Zegaoui, O. *Appl. Catal., A* **1997**, *164*, 91–103.
(11) Birchem, T.; Pradier, C. M.; Berthier, Y.; Cordier, G. *J. Catal.* **1994**, *146*, 503–510.

10.1021/ja8092532 CCC: $40.75

Scheme 2. Hydrogenation Pathways for Crotonaldehyde

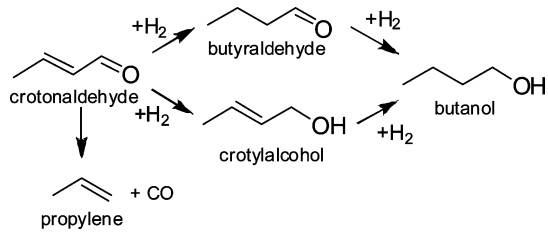

Scheme 3. Hydrogenation Pathways for Prenal

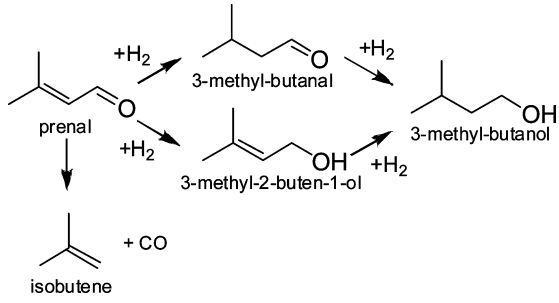

using sum-frequency generation vibrational spectroscopy (SFG-VS) to monitor the surface reaction intermediates. These spectra are then compared to published gas-phase IR spectra, HREEL spectra, and DFT calculations to assist in the interpretation. Crotonaldehyde, with a reaction selectivity that is between that of prenal hydrogenation and acrolein hydrogenation, was chosen to elucidate the effect that catalyst structure has on this reaction. Reaction kinetics using gas chromatography and SFG-VS spectra were taken for crotonaldehyde hydrogenation over Pt(111) and Pt(100) in the temperature range from 150 to 415 K. Finally, prenal hydrogenation was studied kinetically over Pt(111) in the temperature range from 308 to 403 K.

2. Experimental Section

Materials. Crotonaldehyde (99.5%, Fluka) and prenal (97%, Sigma-Aldrich Inc.) were subjected to several freeze−pump−thaw cycles prior to use and their purities were checked by means of gas chromatography and quadrupole mass spectrometry. Acrolein was obtained in gas phase from Airgas with the balance being research grade argon and the purity was verified with quadrupole mass spectrometry to be 99%.

The High-Pressure/Ultrahigh Vacuum System. All experiments reported here were carried out in a high-pressure/ultrahigh vacuum (HP/UHV) system. The UHV chamber is operated at a base pressure of 2×10^{-10} Torr and is isolated from the HP cell by a gate valve. The UHV system is equipped with an Auger electron spectrometer (AES), a quadrupole mass spectrometer (Stanford Research Systems), and an ion bombardment gun (Eurovac). The HP cell consists of two CaF_2 conflat windows that allow transmission of infrared (IR), visible (vis), and sum-frequency radiation for sum-frequency generation (SFG) experiments. The product gases in the HP cell are constantly mixed via a recirculation pump, and kinetic data is acquired by periodically sampling the reaction mixture and analyzing the relative gas phase composition in a flame ionization detector (FID) of a gas chromatograph (Hewlett-Packard HP 5890 on a 5% Carbowax 20 M packed column).

Sample Preparation. Prior to each experiment, the Pt(111) and Pt(100) crystal surfaces were cleaned in the UHV chamber by Ar^+ (1 keV) sputtering for 20 min at approximately 3×10^{-5} Torr of Ar. After sputtering, the crystals were heated to 1103 K in the presence of O_2 of 5×10^{-7} Torr and annealed at the same temperature for 2 min. The cleanliness of the crystal surfaces was verified by AES and the crystallographic structure verified with low-energy electron diffraction (LEED). The samples were then transferred into the HP cell for SFG and kinetic studies.

Sum-Frequency Generation Vibrational Spectroscopy. For SFG measurements, an active/passive mode-locked Nd:YAG laser (Leopard D-20, Continuum) with a pulse width of 20 ps and a repetition rate of 20 Hz was used. The fundamental output at 1064 nm was sent through an optical parametric generation/amplification (OPA/OPG) stage where a tunable IR (2300−4000 cm^{-1}) and a second harmonic vis (532 nm) beam were created. The IR (150 μJ) and vis (200 μJ) beams were spatially and temporally overlapped on the crystal surface at angles of incidence of 55° and 60°, respectively, with respect to the surface normal. The generated SFG beam was collected and sent through a motorized monochromator equipped with a photomultiplier tube to detect the SFG signal intensity. The signal-to-noise ratio was further increased by using a gated integrator while the IR beam was scanned through the spectral region of interest. The SFG signal, I^{SFG}, is related to the incoming visible (I^{vis}) and infrared (I^{IR}) beam intensities, and second-order susceptibility of the media ($\chi^{(2)}$), according to eq 1:

$$I^{SFG}\omega_{SFG} \propto |\chi^{(2)}|^2 I^{vis}\omega_{vis} I^{IR}\omega_{IR} \quad (1)$$

$\chi^{(2)}$ is enhanced when ω_{IR} is at resonance with a vibrational mode of the molecules, q, according to eq 2:

$$I^{SFG} \propto \left|\chi_{NR}{}^{(2)} e^{i\phi_{NR}} + \sum_q \frac{A_q}{\omega_{IR} - \omega_q + i\Gamma_q} e^{i\gamma_q}\right|^2 \quad (2)$$

where $\chi_{NR}{}^{(2)}$ is the nonresonant nonlinear susceptibility, $e^{i\phi_{NR}}$ is the phase associated with the nonresonant background, A_q is the strength of the qth vibrational mode, ω_{IR} is the frequency of the incident IR laser beam, ω_q is the frequency of the qth vibrational mode, Γ_q is the natural line width of the qth vibrational transition, and $e^{i\gamma_q}$ is the phase associated with the qth vibrational transition. All SFG-VS spectra reported are data fit to a form of eq 2.

Since the gas phase in the HP cell absorbs some small amount of the incoming IR radiation, the SFG signal was then normalized by using the following expression (eq 3):

$$I^{SFG,norm} = \frac{I^{SFG}}{\sqrt{I^{IR,before} I^{IR,after}}} \quad (3)$$

where $I^{IR,before}$ and $I^{IR,after}$ define the IR beam intensities measured before and after the HP cell to correct for any infrared radiation absorbed between the HP cell window and the sample, which is mounted exactly halfway between the HP cell entrance and exit window. More information on the HP/UHV system and SFG measurement can be found elsewhere.[12−16]

3. Results and Discussion

3.1. Sum-Frequency Generation Vibrational Spectroscopy of Acrolein, Crotonaldehyde, and Prenal Hydrogenation over Pt(111). 3.1.1. Acrolein Hydrogenation on Pt(111)−SFG-VS Results. Acrolein is the simplest α,β-unsaturated aldehyde, which makes it attractive for surface science study. As can be seen in Scheme 1, it contains only the conjugated carbonyl and alkene groups with no side groups. Using density functional theory analysis, Loffreda et al.[17] examined possible adsorption

(12) Bratlie, K. M.; Flores, L. D.; Somorjai, G. A. *Surf. Sci.* **2005**, *599*, 93–106.
(13) Kung, K. Y.; Chen, P.; Wei, F.; Rupprechter, G.; Shen, Y. R.; Somorjai, G. A. *Rev. Sci. Instrum.* **2001**, *72*, 1806–1809.
(14) Shen, Y. R. *Annu. Rev. Phys. Chem.* **1989**, *40*, 327–350.
(15) Shen, Y. R. *Nature* **1989**, *337*, 519–525.
(16) Yang, M. C.; Tang, D. C.; Somorjai, G. A. *Rev. Sci. Instrum.* **2003**, *74*, 4554–4557.

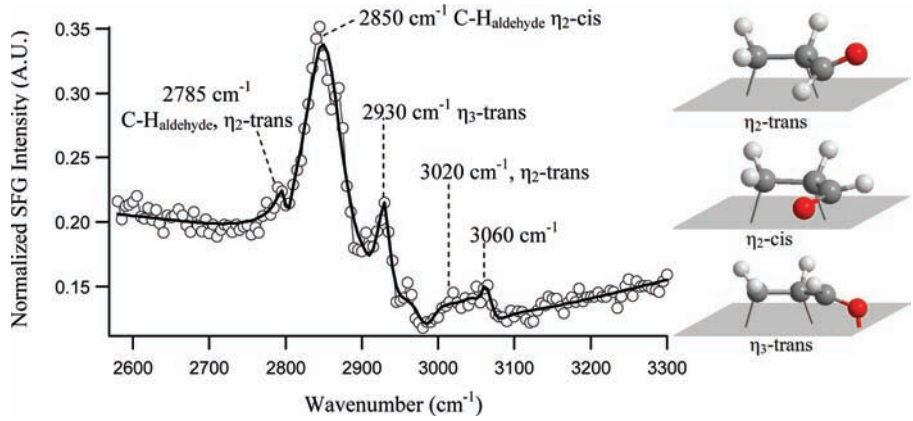

Figure 1. SFG vibrational spectrum of 1 Torr of acrolein in the absence of hydrogen over Pt(111) at 295 K. The aldehyde C−H modes at 2785 and 2850 cm^{-1} clearly identify the presence of η_2-trans and η_2-cis adsorption modes, respectively.

modes of acrolein on Pt(111) at various coverages and determined adsorption energies and predicted a vibrational spectrum for each of the possible stable structures. Experimental assignments of the gas-phase modes of acrolein have been previously published.[18] Further, Murillo et al.[19] examined the adsorption of acrolein to the Pt(111) surface at 110 K using HREELS. Our spectra obtained in situ during the catalytic hydrogenation reactions are compared to the published data.

There are seven stable adsorption modes presented in the theoretical work mentioned above. First, the η_1 adsorption mode has the oxygen atom as the only part of the acrolein molecule that interacts with the Pt(111) surface. The η_2-cis and η_2-trans modes involve a di-σ bond to two Pt atoms originating from the C═C of the acrolein. Clearly, the cis conformer is the one with the oxygen of the carbonyl pointing back toward the acrolein molecule, while in the trans form it points away. The η_3-cis and η_3-trans are the same as the η_2 adsorption modes with the exception that the oxygen atom of the carbonyl is pointing down to and bonding with the metal surface. Finally, the η_4-cis and η_4-trans adsorption modes are bound to the surface via two di-σ bonds, one originating from the C═C and one from the C═O.

Figure 1 shows the SFG vibrational spectrum of 1 Torr of acrolein with no hydrogen added over a Pt(111) single crystal at 295 K. Five vibrational resonances are seen in this C−H region. The vibrational resonance furthest to the red is present at 2785 cm^{-1}, which can be assigned to the aldehyde C−H stretch. The aldehyde C−H in gas-phase acrolein is at 2800 cm^{-1}, so a 15 cm^{-1} red-shift of this clearly identifiable mode occurs upon adsorption. Table 1 gives a direct comparison between the observed SFG-VS vibrational modes and those previously published for acrolein in the literature.

To gain deeper insight into the true bonding characteristics of the acrolein molecule to the Pt(111) surface, the vibrational spectra are compared to those predicted with DFT. Although there are often several structures that correspond to a given vibrational frequency, one can only accept structures if the other peaks in the predicted spectrum also agree with the observed vibrational modes. In the DFT work of Loffreda et al.,[17] the only chemisorption mode of acrolein with a vibrational mode

Table 1. Summary of Experimental Acrolein Vibrational Modes (given in cm^{-1}) for Gas Phase Acrolein,[18] Acrolein Adsorbed onto Pt(111) at 110 K Using HREELS,[19] and the Observed SFG Vibrational Modes for 1 Torr of Acrolein on Pt(111) at 298 K

assignment	IR gas phase	HREELS at 110 K	SFG-VS at 298 K
$\nu_{asym}(=CH_2)$	3103	3098	3060
$\nu(\beta)$(CH)	3069	2997	3020
$\nu_{sym}(=CH_2)$	2998	2908	2930
$\nu_{aldehyde}$(CH)	2800	2854	2850/2785

near this value is the η_2-trans species. The rest of the resonances are seen at 2850, 2930, 3020, and 3060 cm^{-1}. There is a possible shoulder at ~2865 cm^{-1} as well. The η_1 adsorption species, interacting with the Pt surface solely through the oxygen atom, may be ruled out due to the absence of any modes above 3100 cm^{-1} in the SFG-VS spectrum; likewise, the η_4-cis can be eliminated as an option. The mode observed at 2850 cm^{-1} corresponds best with the η_2-cis C−H aldehyde vibrational mode. The two lower frequency aldehyde peaks at 2850 and 2785 cm^{-1} are quite indicative of the η_2 di-σ(CC) adsorption mode, as none of the more highly coordinated surface species have C−H resonances that far to the red.

Figure 2 displays the SFG spectra as 100 Torr of hydrogen is added and the temperature is raised to 415 K. Upon the addition of hydrogen at room temperature, the spectrum undergoes two changes. The small aldehyde peak at 2785 cm^{-1}, corresponding to the η_2-trans surface species, disappears as well as the peak at 3020 cm^{-1}. Due to the fact that those two modes disappear together, as well as the fact that DFT predicts the η_2-trans adsorption mode to have absorptions in both those regions, the 3020 cm^{-1} peak is also assigned to a C−H vibration off of the di-σ bond of the η_2-trans species (Figures 1 and 2), which agrees with the assignment made in the comparison to experimental values in Table 1. Upon heating the Pt(111) crystal to 370 K, a strong new peak appears at 2867 cm^{-1}. The other resonances become very weak and the only one with appreciable signal remains at 2930 cm^{-1}. Upon further heating the Pt(111) crystal to 415 K, the only remaining peak is the 2867 cm^{-1} resonance corresponding to ethylidyne on the surface resulting from the decarbonylation of acrolein. The ethylidyne is red-shifted by about 10 cm^{-1} from its usual location on a clean Pt(111) crystal, but the coadsorption of CO and ethylidyne on Pt(111) has been previously reported to cause a similar red-shift in the ethylidyne peak.[20] The observation of ethylidyne on Pt(111) after acrolein adsorption was also noted by de Jesus and Zaera[21] using RAIRS.

(18) Hamada, Y.; Nishimura, Y.; Tsuboi, M. *Chem. Phys.* **1985**, *100*, 365–375.
(17) Loffreda, D.; Jugnet, Y.; Delbecq, F.; Bertolini, J. C.; Sautet, P. *J. Phys. Chem. B* **2004**, *108*, 9085–9093.
(19) Murillo, L. E.; Chen, J. G. *Surf. Sci.* **2008**, *602*, 919–931.

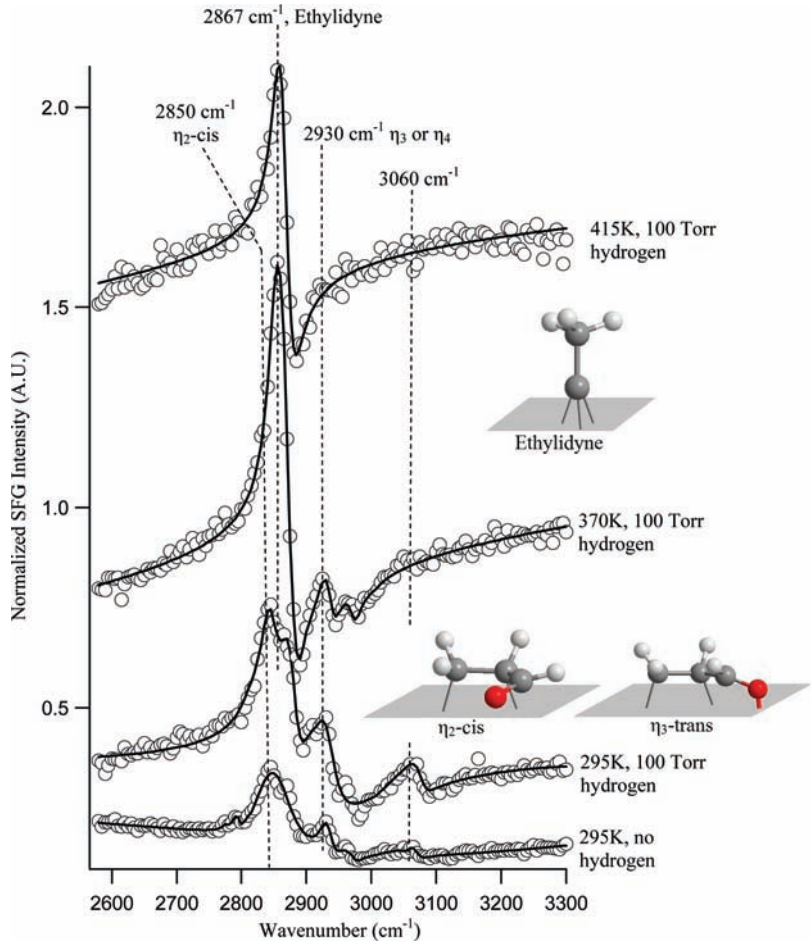

Figure 2. SFG-VS spectra of 1 Torr of acrolein over the Pt(111) crystal surface. The bottom spectra was taken in the absence of hydrogen, and then the subsequent spectra include the addition of 100 Torr of hydrogen and heating the crystal to 415 K. The acrolein peaks vanish and only ethylidyne remains as the crystal is heated.

According to the Gibbs free adsorption energy curves reported by Loffreda et al.[22] for acrolein adsorption to Pt(111), the experimental conditions used here (1 Torr of acrolein, 295−415 K) likely crosses the 0 Gibbs free adsorption energy line as the temperature is raised, thus favoring desorption of the acrolein molecule. This is in agreement with the SFG-VS spectra, as by 415 K the only species remaining on the surface is ethylidyne. Lastly, the peak observed at 2930 cm^{-1} is indicative of a more highly coordinated η_3-trans or η_4-trans surface species. In relation to the DFT calculations, it is most closely matched with the η_3-trans species. Clearly, then, for acrolein adsorption and hydrogenation over Pt(111) there exists a mixed state of adsorption mode surface species.

In a later paper, Loffreda et al.[23] study the hydrogenation reaction pathway with DFT over the Pt(111) surface. Their conclusion was that the reaction actually favors the attack of the C═O carbonyl, but the desorption step of the resulting allyl alcohol has a very high barrier height compared to the reaction pathway involving the attack of the C═C and desorption of the propionaldehyde product. Thus, they conclude that the surface will build up a high concentration of allyl alcohol, but the gas phase will show a high selectivity for the formation of propionaldehyde. In this work, the frequency range from 2500 to 4000 cm^{-1} was studied and there was no evidence found for the unsaturated alcohol on the surface, as was proposed by Loffreda et al.,[23] although a species with the OH bond perfectly parallel to the surface cannot be ruled out due to the metal surface selection rule.[24,25]

3.1.2. Crotonaldehyde Hydrogenation on Pt(111)−SFG-VS Results. The hydrogenation of crotonaldehyde (Scheme 2) has selectivity for the desired unsaturated alcohol between those of acrolein and prenal hydrogenation (section 3.2). The addition of the methyl group improves the selectivity for the unsaturated alcohol, but it also adds complexity to the vibrational spectrum, especially in the C−H region. Figure 3 shows the spectrum for a multilayer of crotonaldehyde on Pt(111) at 150 K in the absence of hydrogen as a reference spectrum, followed by the temperature-dependent spectra of 1 Torr of crotonaldehyde and 100 Torr of hydrogen reacting over a Pt(111) single crystal from 295 to 415 K. In the multilayer (bottom) at 150 K, four vibrational resonances are seen. At 2750 cm^{-1} a strong peak is seen for the trans aldehyde C−H vibration. The analysis of the other three peaks at 2830, 2935, and 2995 cm^{-1} can be made

(20) Chen, P.; Westerberg, S.; Kung, K. Y.; Zhu, J.; Grunes, J.; Somorjai, G. A. *Applied Catalysis A: General* **2002**, *229*, 147–154.
(21) de Jesus, J. C.; Zaera, F. *Surf. Sci.* **1999**, *430*, 99–115.
(22) Loffreda, D.; Delbecq, F.; Sautet, P. *Chem. Phys. Lett.* **2005**, *405*, 434–439.
(23) Loffreda, D.; Delbecq, F.; Vigne, F.; Sautet, P. *Angew. Chem., Int. Ed.* **2005**, *44*, 5279–5282.
(24) Dignam, M. J.; Moskovit, M; Stobie, R. W. *Trans. Faraday Soc.* **1971**, *67*, 3306.
(25) Pearce, H. A.; Sheppard, N. *Surf. Sci.* **1976**, *59*, 205–217.

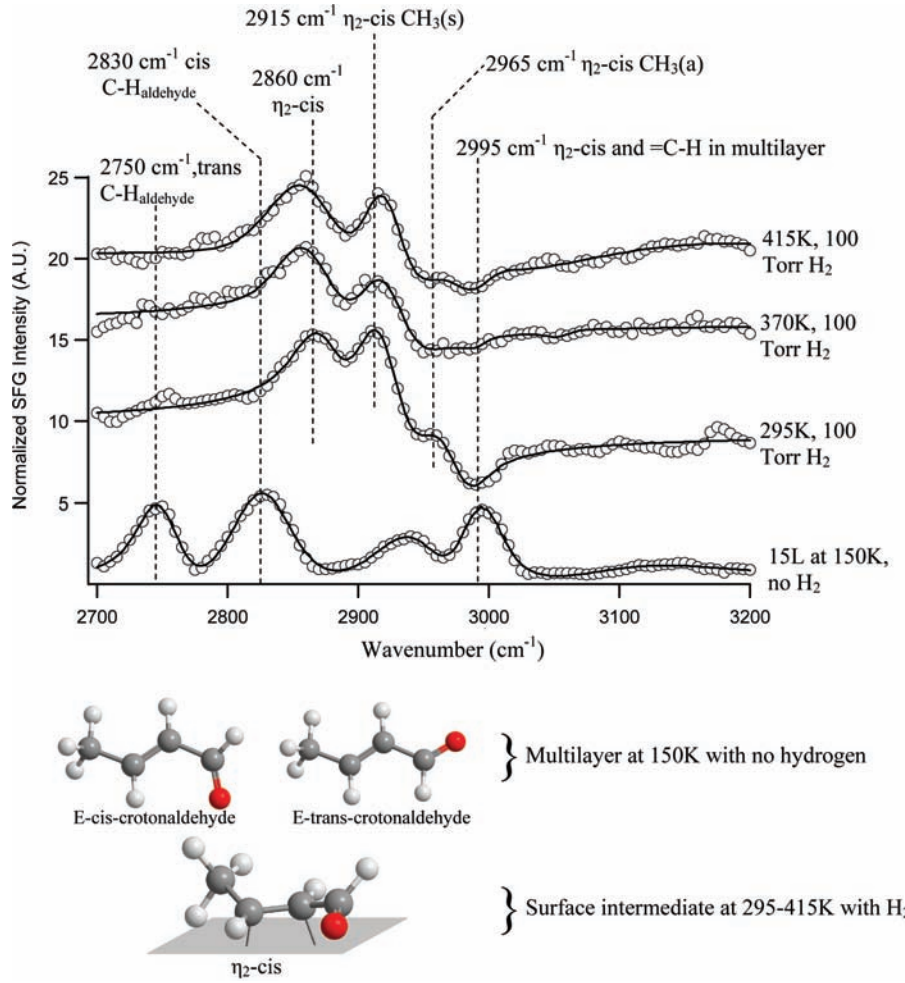

Figure 3. SFG-VS spectra of crotonaldehyde hydrogenation over Pt(111). The bottom spectrum was taken at 150 K after exposing the crystal to 15 L of crotonaldehyde to form a multilayer. The top three spectra were taken with 1 Torr of crotonaldehyde and 100 Torr of hydrogen over the Pt(111) crystal at the temperatures listed.

Table 2. Summary of Experimental Crotonaldehyde Vibrational Modes (given in cm^{-1}) for Gas-Phase Crotonaldehyde[34] and 15 L of Crotonaldehyde Adsorbed to Pt(111) at 150 K Using SFG-VS

assignment	IR gas phase	SFG-VS at 150 K
ν_{asym}(=CH)	3058	2995
ν_{sym}(=CH)	2995	2995
$\nu_{asym}(CH_3)$	2963	2995
$\nu_{sym}(CH_3)$	2938	2935
$\nu_{aldehyde}$(CH)	2805/2728	2830/2750

by comparison to gas-phase IR (Table 2) and DFT calculations[26] for interpretation. In this context, the peak at 2830 cm^{-1} corresponds to the aldehyde C−H stretch of *E*-(*s*)-*cis*-crotonaldehyde, the 2935 cm^{-1} peak corresponds to the symmetric stretching in the methyl side group, and the 2995 cm^{-1} peak corresponds to both the asymmetric methyl stretch and the vinylic C−H stretches of the C=C bond.

The spectrum recorded at 295 K in the presence of hydrogen in Figure 3 shows five vibrational resonances much different from the multilayer condensed onto Pt(111). First, the *trans*-aldehyde C−H stretch around 2750 cm^{-1} disappears by 295 K. Four more resonances are seen at 2865, 2915, 2965, and 2995 cm^{-1}. The 2995 cm^{-1} resonance has flipped from a positive-going peak to a negative-going peak due to a change in its relative phase, as seen in the fit to eq 2. Further, the absence of any peak at 2750 cm^{-1} or below suggests that the η_2-di-σ(CC)-*E*-(*s*)-trans species is not present in significant surface concentration at 295 K in 100 Torr of H_2. Although the trans adsorbed species disappears as the temperature is raised and hydrogen is added, this does not necessarily mean it is no longer participating in the reaction mechanism. The trans species could react more quickly than the cis surface species, in which case no appreciable surface concentration of the trans species would build up.

At 295 K, once again in comparison to the DFT-calculated frequencies,[26,27] the frequencies agree quite well with the η_2-di-σ(CC)-*E*-(*s*)-*cis*-crotonaldehyde species (Figure 3). As the Pt(111) crystal is heated to 415 K, the only notable change is the disappearance of the negative-going peak at 2995 cm^{-1}.

3.1.3. Prenal Hydrogenation on Pt(111)−SFG-VS Results. Figure 4 displays the SFG-VS spectra of 1 Torr of prenal both with and without 100 Torr of hydrogen over Pt(111). A striking difference between these spectra and those discussed for acrolein and crotonaldehyde is the broad −OH hydrogen-bonded peak centered around 3380 cm^{-1} present even before hydrogen is added to the system (made clearer in Figure 5). The hydrogenation of prenal has been shown to be more selective for the

(26) Haubrich, J. Thesis, Universitat Bonn, 2006.

(27) Haubrich, J.; Loffreda, D.; Delbecq, F.; Jugnet, Y.; Sautet, P.; Krupski, A.; Becker, C.; Wandelt, K. *Chem. Phys. Lett.* **2006**, *433*, 188–192.

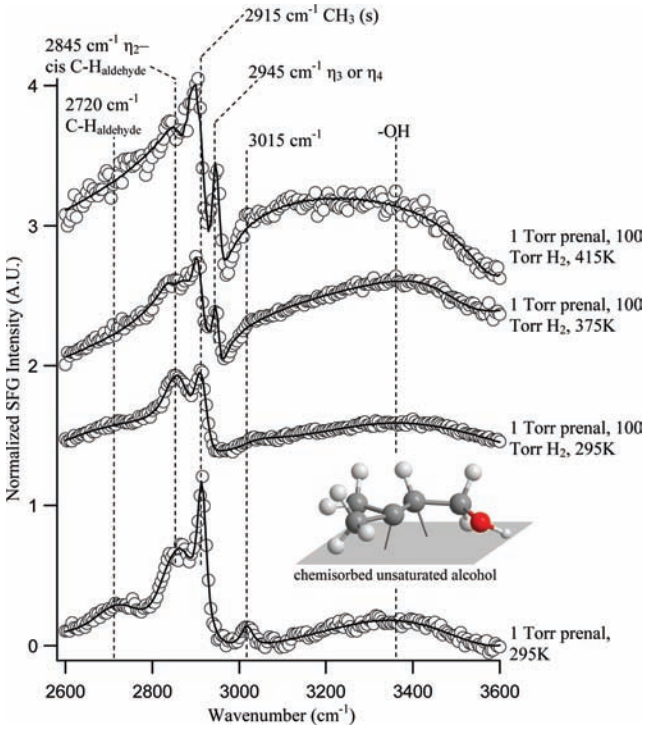

Figure 4. SFG-VS spectra of 1 Torr of prenal over Pt(111) from 295 to 415 K. The bottom one is before the addition of H_2, while the rest are with 100 Torr of H_2. The −OH peak indicates alcohol on the surface at all temperatures. The "soft" modes at 2720 and 2845 cm^{-1} are indicative of η_2 adsorption species. The 2945 cm^{-1} peak is indicative of more highly coordinated η_4 or possibly η_3 adsorbed prenal species.

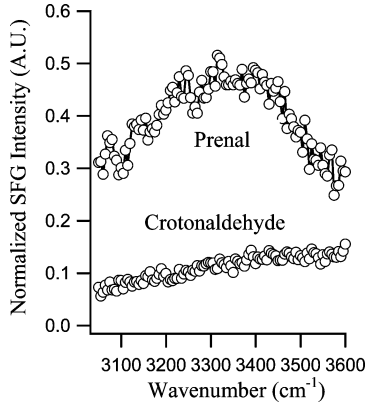

Figure 5. SFG-VS spectra of the −OH region of 1 Torr of prenal on Pt(111) (top) and 1 Torr of crotonaldehyde on Pt(111) (bottom) in the absence of excess hydrogen.

formation of the desired unsaturated alcohol both in previous work[6] and in this work (section 3.3). The buildup of −OH on the surface would indeed indicate that the desorption step of the alcohol is a rate-limiting step, as was proposed for acrolein hydrogenation by Loffreda et al.[23,28] Upon heating, the −OH vibration is red-shifted, indicating a more electron-donating interaction with the surface. This −OH stretch may indicate either the presence of the 3-methyl-2-buten-1-ol product bound to the surface or a hydroxyallyl type reaction intermediate, as proposed by Loffreda et al.,[28] to be in equilibrium with the unsaturated aldehyde reactant. As reported by Haubrich et al.,[29] another possible reaction product in the hydrogenation of prenal is water in a dehydration to form the 3-methylbutane product. The −OH stretch of water cannot be eliminated as a possible source for this observed broad −OH stretch.

Once again, comparing the observed spectra with the DFT-calculated spectra for the various adsorption modes is informative.[26,29,30] For the spectra (Figure 4, bottom and Figure 5, top) taken prior to the addition of hydrogen, a peak is visible at 2720 cm^{-1}, which should clearly correspond to an intact aldehyde C−H. Other than the −OH peak discussed, vibrational peaks are observed at 2845, 2915, and 3015 cm^{-1}. Upon the addition of 100 Torr of hydrogen, the 2720 cm^{-1} peak vanishes and the 3015 cm^{-1} peak becomes much weaker. The only changes in the spectra as the crystal is heated to 415 K is that the −OH band becomes more intense and red-shifted and a new peak grows in at 2945 cm^{-1}. The peak growing in at 2945 cm^{-1} agrees well with the growing presence of either the η_3-di-σ(CC)-σ(O)-(*s*)-cis, corresponding to the asymmetric stretching in one of the methyl groups or to the aldehyde C−H stretch of the η_4-di-σ(CC)-di-σ(CO)-(*s*)-trans species on the surface at higher temperatures. The high temperature spectrum is reversible. After heating to 415 K and then returning the crystal to 295 K, the peak at 2945 cm^{-1} disappears again. This is proof that it is not a cracking product or poison on the surface, but a reversible change in surface intermediate.

3.2. Hydrogenation of Crotonaldehyde over Pt(111) and Pt(100)—Kinetic and SFG-VS Results. The hydrogenation of crotonaldehyde was carried out with 1 Torr of crotonaldehyde and 100 Torr of hydrogen over both the Pt(111) and Pt(100) crystal faces to elucidate the effect that catalyst structure plays in this reaction. The industrially desired product crotyl alcohol, the unsaturated alcohol, results from the hydrogenation of the C═O (Scheme 2), while the thermodynamically favored product, butyraldehyde, results from the hydrogenation of the C═C. Further, the temperature range from 295 to 415 K was used, and apparent activation energies were calculated for the reaction products over both surfaces.

Figure 6 shows the Arrhenius plots and reaction selectivities over both metal surfaces, and Table 3 displays the apparent activation energies for all reaction pathways. The activation energy for the formation of crotyl alcohol is significantly less than that for the formation of butyraldehyde. This is evident also in the reaction selectivities of Figure 5, which show a significantly enhanced selectivity for the formation of the unsaturated alcohol at low temperatures (35 °C). At such low catalytic temperatures, however, the turnover frequencies (TOF, product molecules/Pt site/s) are very low for all products, on the order of 10^{-3}, while as the temperature is raised to 130 °C the TOF for the formation of butyraldehyde approaches $\sim 10^0$ over both surfaces. It is interesting to note that the apparent activation energy for the production of crotyl alcohol is lower than that for the production of butyraldehyde, yet at most temperatures butyraldehyde is the dominant product. The reason for this is 2-fold. First, the reported "apparent" activation energy for crotyl alcohol formation would be underestimated if, for instance, the cracking product resulted only from molecules that first formed crotyl alcohol. In fact, it has been shown that the sticking coefficient for an unsaturated alcohol is significantly

(28) Loffreda, D.; Delbecq, F.; Vigne, F.; Sautet, P. *J. Am. Chem. Soc.* **2006**, *128*, 1316–1323.
(29) Haubrich, J.; Loffreda, D.; Delbecq, F.; Sautet, P.; Jugnet, Y.; Krupski, A.; Becker, C.; Wandelt, K. *J. Phys. Chem. C* **2008**, *112*, 3701–3718.
(30) Hirschl, R.; Delbecq, F.; Sautet, P.; Hafner, J. *J. Catal.* **2003**, *217*, 354–366.

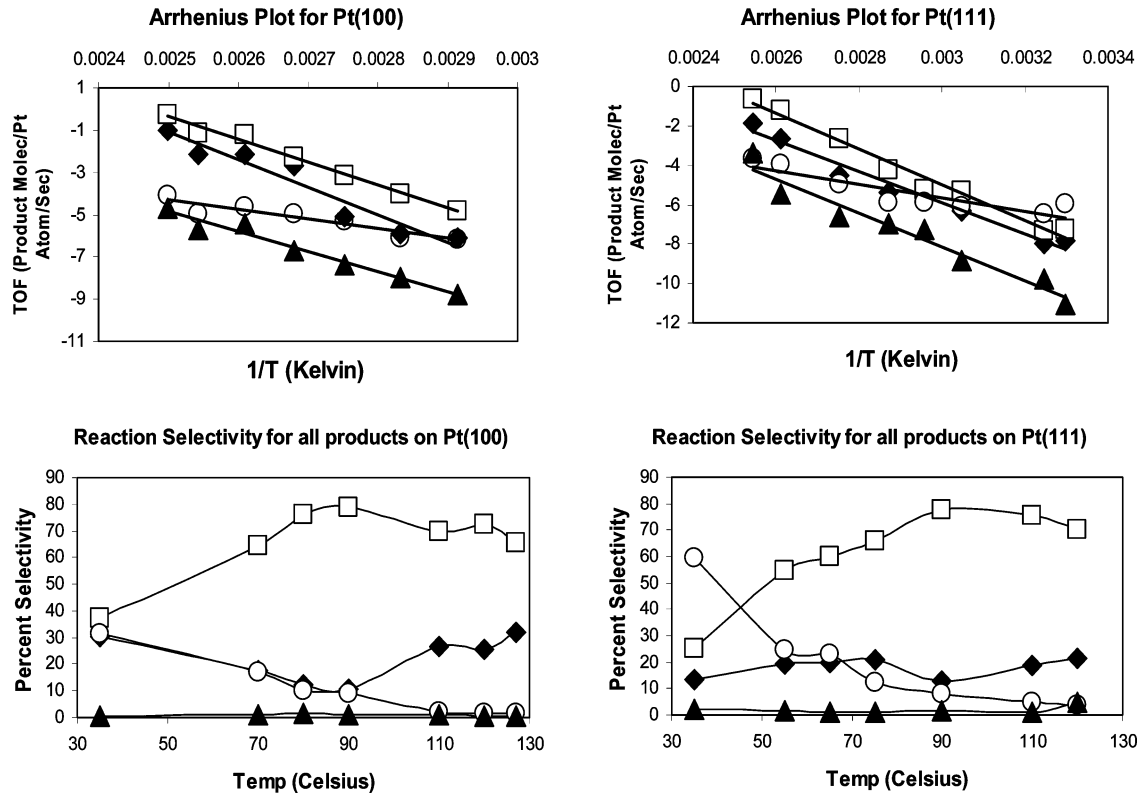

Figure 6. Arrhenius plots (top) and reaction selectivities (bottom) taken once a steady state was reached for the hydrogenation of crotonaldehyde over Pt(111) (right) and Pt(100) (left). The major reaction products are butyraldehyde (□), crotyl alcohol (○), propylene (◆), and butanol (▲).

Table 3. Activation Energies in kJ/mol for the Various Products of Crotonaldehyde Hydrogenation Carried out over Pt(111) and Pt(100) with 1 Torr of Crotonaldehyde and 100 Torr of Hydrogen

	Pt(111)	Pt(100)
butyraldehyde	75	90
crotyl alcohol	35	38
propylene	68	63
butanol	59	79

higher than its corresponding saturated aldehyde,[11] which may lead to longer residence times and further reactions, such as decarbonylation. Second, the pre-exponential factors for the two reaction pathways could conceivably be different. Given that there may exist more than one adsorption mode of the crotonaldehyde molecule on the Pt(111) surface, it is reasonable that one adsorption mode may favor the formation of crotyl alcohol while another favors the formation of butyraldehyde, changing their associated reaction entropies.

Pt(111) shows a higher selectivity for the formation of the unsaturated alcohol, especially at low temperatures, while Pt(100) shows a higher selectivity for the formation of the decarbonylation "cracking" product propylene (Figure 6). The selectivity for the totally saturated product butanol remained low, less than 1%, on both surfaces at the temperatures studied.

Similar to the results reported by Lawrence and Schreifels,[31] the selectivity for the formation of the desired unsaturated alcohol, crotyl alcohol, varied with time. Figure 7 shows the time dependence for the hydrogenation of 1 Torr of crotonaldehyde with 100 Torr of hydrogen for 2 h at 90 °C. Initially, the selectivity for the formation of crotyl alcohol is as high as 45%, but by the time the reaction reaches a steady-state product distribution the crotyl alcohol selectivity has dropped to ~10%. This change in selectivity may be due to either the selective blocking of active sites by CO during the decarbonylation of crotonaldehyde or by carbonaceous deposits, both of which have previously been reported to deactivate this reaction over model Pt nanoparticle catalysts.[32] This gives a further reason why the reaction appears to shift to favor crotyl alcohol production at low temperatures. At lower temperatures the deactivation mechanism which causes the shift in selectivity with time may be less active. STM experiments are currently underway to help elucidate this effect.

Figure 8 compares a spectrum taken over Pt(111) to one taken over Pt(100) under 1 Torr of crotonaldehyde and 100 Torr of hydrogen at 295 K. The vibrational features between the two crystal faces were identical here and for all temperatures studied. This argues that the dominant surface reaction intermediates are the same for both crystal faces for the hydrogenation of crotonaldehyde. This is in contrast to theoretical work done by Delbecq et al.,[33] which demonstrated significantly different adsorption modes for crotonaldehyde between the Pt(111) and Pt(100) surfaces. However, it is consistent with the reaction selectivities and kinetics above which demonstrated very similar activities and selectivities for the two surfaces, the primary difference simply being in the barrier heights for the various reaction pathways evidenced by the differing activation energies calculated allowing for some kinetic control of the product distribution.

(31) Lawrence, S. S.; Schreifels, J. A. *J. Catal.* **1989**, *119*, 272–275.
(32) Grass, M.; Rioux, R.; Somorjai, G. *Catal. Lett.* **2009**, *128*, 1–8.
(33) Delbecq, F.; Sautet, P. *J. Catal.* **1995**, *152*, 217–236.
(34) Oelichmann, H. J.; Bougeard, D.; Schrader, B. *J. Mol. Struct.* **1981**, *77*, 179–194.

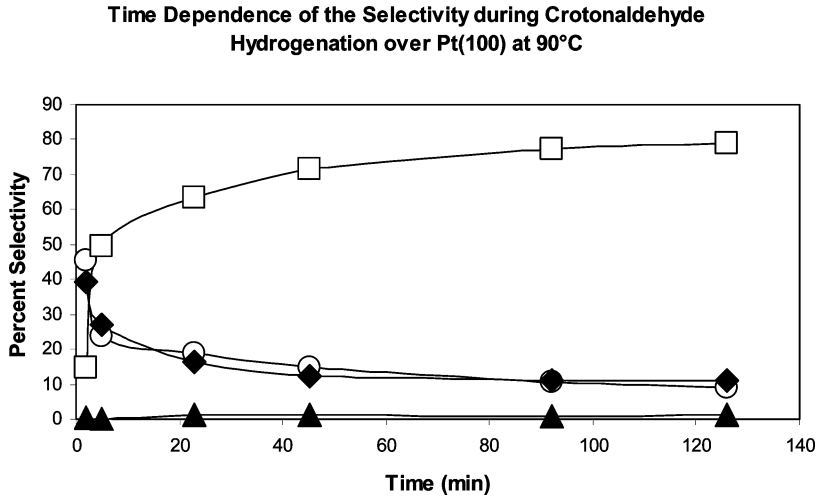

Figure 7. Product selectivities in the hydrogenation of crotonaldehyde (1 Torr of crotonaldehyde/100 Torr of hydrogen) at 90 °C. The major reaction products are butyraldehyde (□), crotyl alcohol (○), propylene (◆), and butanol (▲). A dramatic change in reaction selectivity is seen during the first 20 min and a steady-state product distribution is reached at around 2 h.

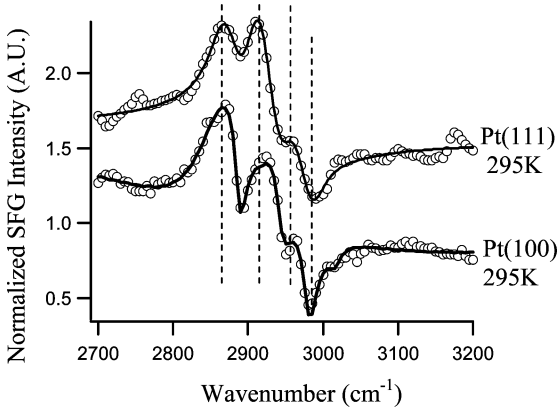

Figure 8. SFG-VS spectra of 1 Torr of crotonaldehyde and 100 Torr of hydrogen at 295 K over Pt(100) (bottom) and Pt(111) (top). SFG-VS spectra over Pt(111) and Pt(100) showed identical features at all temperatures from 295 to 415 K.

3.3. Hydrogenation of Prenal over Pt(111)—Kinetic Results. For comparison to the results obtained for the hydrogenation of crotonaldehyde, the hydrogenation of prenal was carried out over Pt(111) over the temperature range from 35 to 130 °C under 1 Torr of prenal and 100 Torr of hydrogen. The addition of the extra methyl group (Scheme 3) to the C═C bond adds steric hindrance to the adsorption of this moiety, and thus may increase the selectivity to the unsaturated alcohol product. Figure 9 displays the time dependence of the reaction selectivity for prenal hydrogenation over Pt(111) at 70 °C for 2.5 h. The initial reaction selectivity was 100% for the production of the desired unsaturated alcohol, but the reaction selectivity reached a steady state at about 1.5 h and the production of unsaturated alcohol had fallen to 33% by this time.

As can be seen in Figure 10, the selectivity for the formation of unsaturated alcohol at 100 °C was 37%. This is more than 5 times higher than the selectivity for the unsaturated alcohol during crotonaldehyde hydrogenation at this temperature. As the temperature is raised to 130 °C, however, the onset of cracking product formation appears to come at the cost of unsaturated alcohol production. The selectivity for 3-methyl-2-buten-1-ol drops to ∼10% at this temperature as the selectivity for the cracking products concomitantly rises. To obtain the reaction selectivity at 35 °C, the reaction was allowed to proceed for 14 h. The only major detectable product was the desired unsaturated alcohol; however, this effect may be somewhat exaggerated as the reaction may not have yet reached its final steady-state product distribution.

4. Conclusions

Using a combination of SFG vibrational spectroscopy and kinetic measurements, along with detailed comparison to published IR, HREELS, and DFT calculations, the surface species during the catalytic hydrogenation of acrolein, crotonaldehyde, and prenal have been clarified. The effect that catalyst structure has on the hydrogenation of crotonaldehyde has been elucidated by comparing both the reaction kinetics and SFG-VS spectra over Pt(111) and Pt(100) single crystals.

In the case of acrolein, a mixed adsorption state existed including η_2-cis and η_2-trans species, as well as more highly coordinated η_3 or η_4 species. However, upon the addition of hydrogen, the η_2-trans surface species vanished. Further, as the Pt(111) crystal was heated to 415 K, all of the surface intermediate peaks vanished, except that of ethylidyne, forming from the decarbonylation of acrolein.

The reaction kinetics for crotonaldehyde hydrogenation showed a lower activation energy for the formation of the industrially desired crotyl alcohol than for the formation of the thermodynamically favored butyraldehyde. Thus, at lower temperatures the selectivity for the desired product was enhanced.

For the adsorption of crotonaldehyde to Pt(111) at 150 K, both cis and trans species were found with SFG-VS. However, in the presence of hydrogen at 295 K and hotter, the only surface species observed was η_2-cis. This may be an indication that the η_2-trans species is not stable at the higher temperature or is simply the fastest one to react and desorb, not allowing a significant surface concentration to build up. The SFG-VS data, then, agree nicely with the reaction kinetics, given that the η_2 adsorption modes do not have the carbonyl interacting with the surface and the selectivity for the hydrogenation of the C═O was low in the case of crotonaldehyde hydrogenation.

Pt(111) and Pt(100) showed little structure sensitivity for this reaction. The Pt(111) had a somewhat higher selectivity for the formation of crotyl alcohol, while Pt(100) had a higher

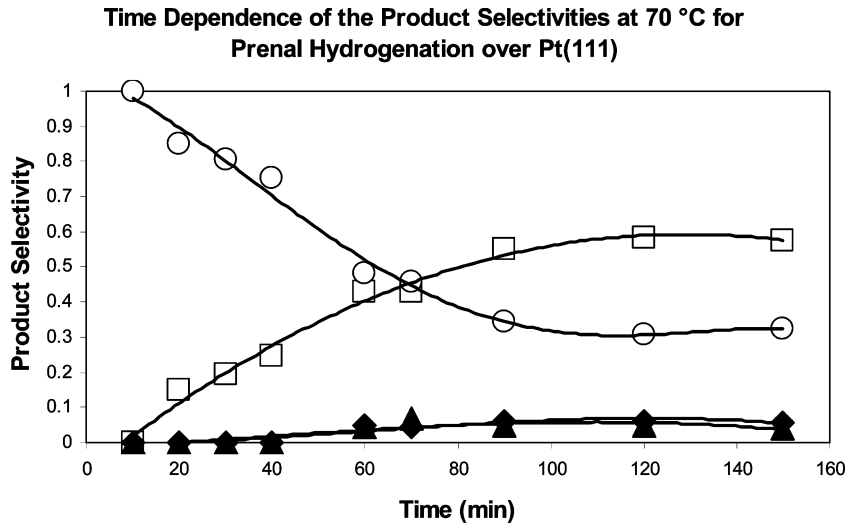

Figure 9. Product selectivities as a function of time for prenal hydrogenation over Pt(111) using 1 Torr of prenal and 100 Torr of hydrogen. Initial selectivity was 100% for the unsaturated alcohol, but as the reaction progressed to a steady state after about 2 h, the selectivity for the unsaturated alcohol fell to 33%. The major reaction products are 3-methylbutyraldehyde (□), 3-methyl-2-buten-1-ol (○), C_4 cracking products (◆), and 3-methylbutanol (▲).

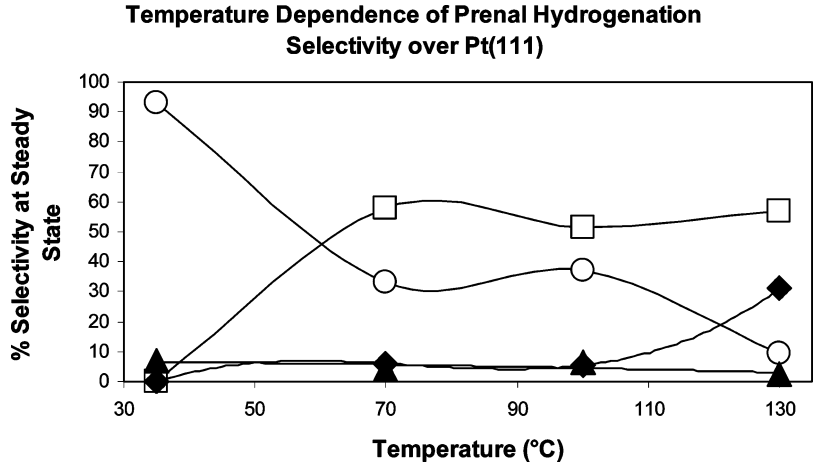

Figure 10. Product selectivities during the hydrogenation of prenal over Pt(111) as a function of temperature. All selectivities were taken once a steady state had been reached, typically about 2 h into the reaction. At 35 °C, the data points were taken at 14 h. The major reaction products are 3-methylbutyraldehyde (□), 3-methyl-2-buten-1-ol (○), C_4 cracking products (◆), and 3-methylbutanol (▲).

selectivity for the decarbonylation "cracking" reaction. Further, the SFG-VS spectra of crotonaldehyde hydrogenation over both surfaces were identical.

For the hydrogenation of prenal over Pt(111), the SFG-VS results indicated the presence of an −OH group, even without the presence of excess hydrogen. This is consistent with the flipped selectivity for the hydrogenation of prenal, in which the dominant product is the unsaturated alcohol. SFG-VS spectra demonstrated the presence of the η_2 surface species definitively. Further, upon heating the Pt(111) crystal to 415 K, a highly coordinated η_3 or η_4 species grows in on the surface. This clear difference from crotonaldehyde also agrees with the difference in reaction selectivities. The C═O of prenal interacts with the surface at higher temperatures, unlike the case for crotonaldehyde, and the C═O is hydrogenated significantly more during prenal hydrogenation than crotonaldehyde hydrogenation.

Acknowledgment. This work was supported by the Director, Office of Energy Research, Office of Basic Energy Sciences, and Materials Sciences Division of the U.S. Department of Energy under Contract DE-AC02-05CH11231. M.B. thanks the Swiss National Science Foundation (SNF) for financial support.

JA8092532